P H Y S I C A L   R E V I E W   L E T T E R S

Clustering of Nonergodic Eigenstates in Quantum Spin Glasses

C. L. Baldwin,[1,2] C. R. Laumann,[1] A. Pal,[3] and A. Scardicchio[4,5]

[1]*Department of Physics, Boston University, Boston, Massachusetts 02215, USA*
[2]*Department of Physics, University of Washington, Seattle, Washington 98195, USA*
[3]*Rudolf Peierls Centre for Theoretical Physics, Oxford University, Oxford OX1 3NP, United Kingdom*
[4]*Abdus Salam ICTP Trieste, Strada Costiera 11, 34151 Trieste, Italy*
[5]*INFN, Sezione di Trieste, Via Valerio 2, 34127 Trieste, Italy*

The two primary categories for eigenstate phases of matter at a finite temperature are many-body localization (MBL) and the eigenstate thermalization hypothesis (ETH). We show that, in the paradigmatic quantum *p*-spin models of the spin-glass theory, eigenstates violate the ETH yet are not MBL either. A mobility edge, which we locate using the forward-scattering approximation and replica techniques, separates the nonergodic phase at a small transverse field from an ergodic phase at a large transverse field. The nonergodic phase is also bounded from above in temperature, by a transition in configuration-space statistics reminiscent of the clustering transition in the spin-glass theory. We show that the nonergodic eigenstates are organized in clusters which exhibit distinct magnetization patterns, as characterized by an eigenstate variant of the Edwards-Anderson order parameter.

Many systems under experimental investigation as platforms for many-body localization (MBL) [1–9] have long-range interactions that mediate the direct transport of excitations. This includes disordered electronic materials [10,11], ion traps [12], interacting nitrogen-vacancy centers in diamond [13,14], and superconducting qubit devices developed for adiabatic quantum computing [15–17]. In sufficiently long-ranged systems, the proliferation of long-distance resonances precludes quantum mechanical localization [18–22], an intuitive result strongly supported by analytic work over the past half century. Nevertheless, the quantum random energy model (QREM), an infinite-range spin glass, was recently shown to exhibit a phase with localized eigenstates at a finite energy density [23,24]. The QREM provides an analytically tractable framework for studying mobility edges and configuration-space localization. This raises the obvious question of how localization survives despite the infinite-range interactions and what role it plays in more realistic long-range systems.

Some insight comes from considering the distribution of local fields—i.e., the energy required to flip one of the system's N spins relative to a given configuration. In the QREM, flipping a spin typically changes the energy by $O(N)$. Thus, the quantum fluctuations which lead to the proliferation of resonances are strongly suppressed. However, short-range models have $O(1)$ local fields, and, in fact, so do power-law and infinite-range systems with general *p*-body interactions. This suggests that the eigenstate-localized phase of the QREM is an exceptional case among long-range models: Strict configuration-space localization cannot exist in any model with $O(1)$ local fields, since the introduction of quantum dynamics causes resonant fluctuations.

In this Letter, we study the eigenstate properties of the quantum *p*-spin models [25–28]. Over the past four decades, these models have become paradigms for the mean-field theory of spin glasses [29–32], particularly the Sherrington-Kirkpatrick model ($p = 2$) [33,34]. The QREM corresponds to the $p \to \infty$ limit in many senses, but the local-field distribution remains $O(1)$ in any finite-*p* model. Consequently, the QREM's phase of localized eigenstates gives way to a phase of delocalized yet nonergodic eigenstates (blue in Fig. 1), similar to what was observed in the context of single-particle localization on the Bethe lattice [35–37]. This is in contrast to the fully delocalized paramagnetic phase (orange in Fig. 1), in which eigenstates satisfy the eigenstate thermalization hypothesis (ETH) [38–40] and exhibit thermal behavior.

The formal distinction that we make between ergodic, nonergodic, and MBL eigenstates concerns the off-diagonal matrix elements of local operators between them. Schematically, denote by $\hat{\sigma}$ any operator supported on $O(1)$ spins and consider the state $\hat{\sigma}|\Psi\rangle$ (with $|\Psi\rangle$ an eigenstate). According to the ETH [41], the overlap with any other eigenstate $|\Phi\rangle$ at the same energy density ϵ should scale as $\langle\Phi|\hat{\sigma}|\Psi\rangle \sim \{1/\sqrt{\exp[Ns_{eq}(\epsilon)]}\}g(\epsilon, E_\Psi - E_\Phi)$, where $s_{eq}(\epsilon)$ is the thermodynamic entropy density and g is a smooth function of ϵ and the energy difference. Our analysis below suggests that the eigenstates of the ETH phase in Fig. 1 obey this scaling. On the other hand, in a MBL phase $\hat{\sigma}|\Psi\rangle$ should have significant weight only on $O(1)$-many eigenstates [2], a notion one can make precise through a participation ratio [e.g., $\sum_\Phi |\langle\Phi|\hat{\sigma}|\Psi\rangle|^4 \sim O(1)$]. We find that the eigenstates of the nonergodic phase *do not* obey this definition of MBL, even though they violate the ETH.
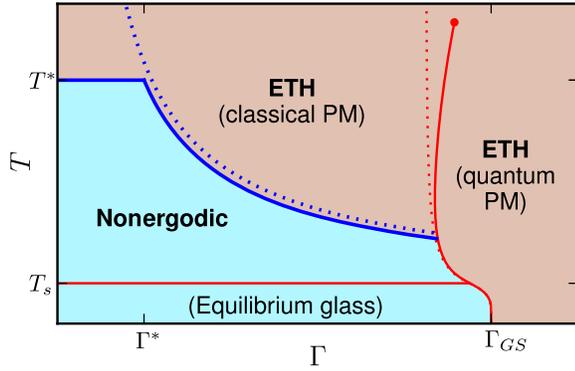
FIG. 1. The $T - \Gamma$ phase diagram of the quantum p-spin model, sketched for arbitrary p. The indicated T and Γ values scale as $T_s = O(1)$, $T^* \simeq \sqrt{(p/4\ln p)}$, $\Gamma^* \simeq \sqrt{(\ln p/p)}$, and $\Gamma_{GS} = O(1)$. Solid red lines are phase boundaries obtained through the imaginary-time replica formalism [25], and the solid blue line is the eigenstate phase boundary. The corresponding dashed red and blue lines are those of the QREM ($p \to \infty$ limit).

Rather, they are organized into "clusters" (defined below). Within a cluster c, eigenstates follow ETH-type scaling:

$$\langle \Phi^{(c)} | \hat{\sigma} | \Psi^{(c)} \rangle \sim \frac{1}{\sqrt{\exp\left[N s_c(\epsilon) \right]}} g_c(\epsilon, E_\Psi - E_\Phi), \quad (1)$$

but off-diagonal matrix elements between clusters are heavily suppressed ($c \neq c'$):

$$\langle \Phi^{(c')} | \hat{\sigma} | \Psi^{(c)} \rangle \ll \frac{1}{\sqrt{\exp\left[N s_{\mathrm{eq}}(\epsilon) \right]}}. \quad (2)$$

Here, $| \cdot {}^{(c)} \rangle$ and $| \cdot {}^{(c')} \rangle$ are eigenstates belonging to each cluster. $s_c(\epsilon)$ is the entropy density within c [which is strictly less than $s_{\mathrm{eq}}(\epsilon)$], and g_c is a smooth, cluster-dependent $O(1)$ function. More physically, such nonergodic eigenstates are thermal within a cluster but not thermal in the configuration space as a whole.

Concretely, the quantum p-spin models are defined by

$$H_p = -\sum_{(i_1 \dots i_p)} J_{i_1 \dots i_p} \hat{\sigma}_{i_1}^z \dots \hat{\sigma}_{i_p}^z - \Gamma \sum_{i=1}^{N} \hat{\sigma}_i^x \equiv H_p^C + H^Q, \quad (3)$$

where the classical term H_p^C sums over all distinct p-tuples of N spins and the quantum term H^Q provides a uniform transverse field. The random couplings $J_{i_1 \dots i_p}$ are independent identically distributed Gaussians of mean 0 and variance $(p!/2N^{p-1})$, to ensure extensivity. It is known [25] that the thermodynamic free energy of H_p approaches that of the QREM as p increases. The eigenstate phases of H_p do as well, yet the eigenstates are never localized at any finite p. They are instead nonergodic, in a manner that comes to resemble localization as p increases. We show this by studying the eigenstates within the perturbation theory and the forward-scattering approximation [42].

Before we turn to a detailed analysis, it is useful to consider the p-spin models in terms of Anderson localization on the N-dimensional hypercube defined by the σ^z configuration space. H_p^C is then a random potential, and H^Q causes hops along the edges of the hypercube. The QREM corresponds to an uncorrelated Gaussian random potential of bandwidth $\sqrt{N}$. This bandwidth models that of a many-body system with an extensive spectrum, but the lack of correlations implies unrealistically large local fields. In the p-spin model, the potential remains Gaussian but exhibits correlations which restrict the energy differences between adjacent sites to be $O(p)$. This leads to the entropically large clusters over which the eigenstates delocalize at a short fractional Hamming distance (see below). The phase transition at a finite transverse field shown in Fig. 1 corresponds to eigenstates tunneling *between* clusters. To obtain the eigenstates, we must first consider the correlations in the classical energy landscape in more detail. At Hamming distance Nx from a given configuration with energy $N\epsilon_0$, the Gaussian random potential obeys a conditional distribution [29]

$$P_x(\epsilon) \propto \exp\left(-N \frac{[\epsilon - (1 - 2x)^p \epsilon_0]^2}{1 - (1 - 2x)^{2p}} \right). \quad (4)$$

Intuitively, configurations at distance $x \lesssim (1/p)$ have similar energies and reduced fluctuations relative to independently sampled states, as a result of the $O(1)$ local fields. See Ref. [43], Sec. B, for more details.

Using Eq. (4), the average number of states at fractional distance x with energy density ϵ matching ϵ_0 is $\binom{N}{Nx} P_x(\epsilon_0) \sim e^{Ns(x)}$, with

$$s(x) = -x \ln x - (1 - x) \ln (1 - x) - \frac{1 - (1 - 2x)^p}{1 + (1 - 2x)^p} \epsilon_0^2. \quad (5)$$

In order to compare with the literature, it is useful to parametrize ϵ_0 through the temperature T defined by a formal Legendre transform, even when the system fails to thermalize dynamically. It is shown in Ref. [43], Sec. A, that $\epsilon_0 = -(1/2T) + O(1/p^2)$. Equation (5) is an annealed average which provides a rigorous upper bound for the typical number of states, since $\mathbb{E}[\ln \dots] \leq \ln \mathbb{E}[\dots]$. When $s(x) < 0$, we know with certainty that there are no configurations at x with energy density ϵ_0.

The entropy $s(x)$ is plotted in Fig. 2 for $p = 6$ as an illustration. A transition occurs at the temperature T^*. At $T > T^*$, there are configurations over the entire range of x, whereas at $T < T^*$, there is a "forbidden" region $(x^*(T), x^{**}(T))$ in which no configurations lie. We have rigorously confirmed the presence of three distinct regions via a second-moment analysis, analogous to that done in Ref. [44]. See Ref. [43], Sec. D, for details. Thus, the configurations at energy ϵ_0 form disconnected clusters of
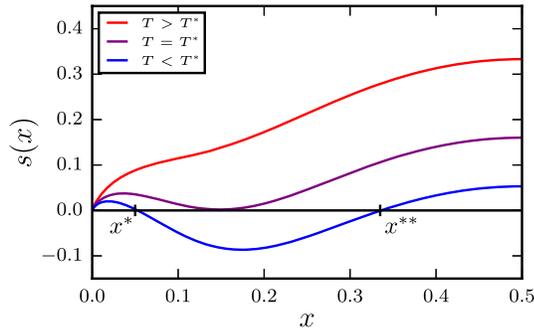
FIG. 2.   The annealed Hamming-distance-resolved entropy $s(x)$ (for $p = 6$). x is the fractional Hamming distance relative to a configuration conditioned to have energy density $\epsilon_0 = -(1/2T)$. Note that these curves are for $\Gamma = 0$. Red curve, $T = 0.83$. Purple curve, $T = 0.69$. Blue curve, $T = 0.63$.

Hamming size $x^*(T)$. Energy levels within a cluster are highly correlated, but those of different clusters are essentially independent [see Eq. (4)]. This behavior is analogous to the clustering observed in, e.g., k-SAT problems [44], coloring of random graphs [45], and the replica theory of spin glasses [46,47].

By setting $s(x) = \partial_x s(x) = 0$, we find that

$$T^* = \sqrt{\frac{p}{4 \ln p}} \left[1 + O\left(\frac{\ln \ln p}{\ln p} \right) \right]. \qquad (6)$$

Note that $T^* \to \infty$ as $p \to \infty$. Furthermore, at $T \ll T^*$, $x^*(T) \sim e \exp \left[-(1/4T^2)p \right]$, whereas $x^{**}(T) \sim O(1)$ (with respect to p). Thus, the clusters below T^* are well separated, and they become arbitrarily small as p increases. Regardless, the clusters cover a macroscopic Hamming distance at any finite p.

With this understanding of how the *classical* states at energy density ϵ_0 are organized, we now introduce a small transverse field Γ and study the eigenstates within the perturbation theory. Let $|\Psi_\alpha\rangle$ be the eigenstate that results from perturbing the classical configuration $|\alpha\rangle$, and let $|\beta\rangle$ be another classical state separated by Hamming distance Nx. Since the perturbation $-\Gamma \sum_i \hat{\sigma}_i^x$ flips a single spin at each order, the leading nonzero contribution to $\langle \beta | \Psi_\alpha \rangle$ arises at the Nxth order. In the forward-scattering approximation (FSA), we retain only this contribution for each configuration $|\beta\rangle$. Note that many terms nonetheless contribute to $\langle \beta | \Psi_\alpha \rangle$: one for each of the $(Nx)!$ distinct *sequences* of spin flips that transform $|\alpha\rangle$ into $|\beta\rangle$. Thus, within the FSA,

$$\langle \beta | \Psi_\alpha \rangle \approx \frac{\Gamma}{E_\alpha - E_\beta} \sum_{\mathcal{P}} \prod_{\gamma \in \mathcal{P}} \frac{\Gamma}{E_\alpha - E_\gamma}. \qquad (7)$$

The sum runs over the sequences $\mathcal{P}$, and the product runs over each intermediate configuration $|\gamma\rangle$ along sequence $\mathcal{P}$.

Note that Eq. (7) is indeed Nxth order in Γ. See [24,42] for more explicit derivations.

Before turning to a quantitative analysis of Eq. (7), let us sketch the key ideas. Even for small Γ, the amplitude $\langle \beta | \Psi_\alpha \rangle$ can be large if the denominators in Eq. (7) are small. We will find that such "resonances" show up at small distances x regardless of T (i.e., $\epsilon_0 \equiv E_\alpha / N$) and Γ. The large amplitudes appear to invalidate our perturbative expansion. However, a more accurate treatment regulates them by introducing self-energy corrections [18]. Furthermore, for $T < T^*$ there is the tunneling region (x^*, x^{**}) in which resonances cannot exist (see Fig. 2). Here the self-energy corrections are negligible. Thus, the naïve FSA accurately estimates the suppression of amplitude due to tunneling through this forbidden region. If it predicts that *every* amplitude at $x > x^{**}$ is exponentially suppressed, then we know that the eigenstates do not delocalize across the forbidden region and are nonergodic. There turns out to be a critical $\Gamma_c(T)$ below which eigenstates are nonergodic in precisely this sense.

Rather than introducing self-energies, an alternative approach to account for the short-distance resonances is the degenerate perturbation theory. Although precise calculations along these lines are infeasible, we expect the resulting eigenstates to have amplitudes uniformly distributed across all resonant configurations, as in the random matrix theory. Restarting the perturbation theory from these hybridized states leads to new resonances which must themselves be included in the degenerate perturbation theory, leading to yet further resonances, and so on. At $T < T^*$, this process terminates when all degenerate states at $x < x^*$ have been incorporated. We accordingly expect the eigenstates to appear thermal *with respect to* this short-distance cluster [cf. Eq. (1)]. If $\Gamma < \Gamma_c(T)$, the eigenstates are nonetheless nonergodic for the reasons outlined above. Yet, if $\Gamma > \Gamma_c(T)$, we find further resonances in other clusters. Since these states hybridize not just within but *between* clusters, we expect them to be fully ergodic. Similarly, at $T > T^*$ there is no forbidden region and nothing prevents every configuration at T from hybridizing. Here we expect full ergodicity at any Γ. This is illustrated in Fig. 1.

We now quantitatively demonstrate the existence of the nonergodic phase at $T < T^*$ and locate its phase boundary $\Gamma_c(T)$. Specifically, we count the number of resonant configurations β at distance x, i.e., those that have $|\langle \beta | \Psi_\alpha \rangle| \geq A$, where A is any $O(1)$ number. We evaluate the sum over paths in Eq. (7) using a replica analysis (see [43], Secs. E and F), [46] to find its typical behavior. When $|E_\alpha - E_\beta|$ is less than the resulting tunneling amplitude, β is resonant. The expected number of resonances at distance x is then given by $e^{Nf(x)}$ (see [43], Sec. F), where

$$f(x) = \underbrace{\int_0^x dy \ln \frac{1}{1-(1-2y)^p} + x \ln \frac{x\Gamma}{e|\epsilon_0|}}_{\text{typical value of the sum in Eq. (7)}} \underbrace{-x \ln x - (1-x) \ln (1-x) - \frac{1-(1-2x)^p}{1+(1-2x)^p}\epsilon_0^2}_{\text{number of degenerate configs. at } x \text{ [i.e., } s(x)]}. \tag{8}$$

Analogous to $s(x)$, $f(x) < 0$ means that every configuration at distance x has an amplitude that vanishes with certainty as $N \to \infty$.

Figure 3 shows the three different qualitative behaviors of $f(x)$ as T and Γ are varied. Each corresponds to one of the cases described above. For $T \ll T^*$ (bottom two curves, Fig. 3), there are resonances at $x < x^*$, belonging to the same cluster (see the inset). Resonances belonging to different clusters appear only when Γ exceeds a critical $\Gamma_c(T)$ (middle curve). In line with the comments above, we should treat the intracluster resonances via the degenerate perturbation theory before considering larger distances. However, since intracluster resonances cannot extend past $x^* \ll O(1)$, this effect gives only subleading corrections to the number of resonances in other clusters. At $T > T^*$ (top curve), one can no longer define separate clusters, and we find resonances throughout the configuration space. The FSA is certainly not valid in this regime—it merely confirms the consistency of our results.

It is straightforward to determine $\Gamma_c(T)$ from Eq. (8): It is defined by where the maximum of $f(x)$ over all $x > x^*(T)$ is 0. The result (see [43], Sec. F), is the portion of the blue curve below T^* in Fig. 1. To within $O(1/p)$ corrections, it is identical to that of the QREM [24]. Since T^* diverges as p increases, we find that the nonergodic phase of H_p does indeed map continuously onto the MBL phase of H_{QREM}.

The fact that eigenstates at low T and small Γ are nonergodic has important consequences for their properties, many of which are commonly associated with MBL. One prominent obs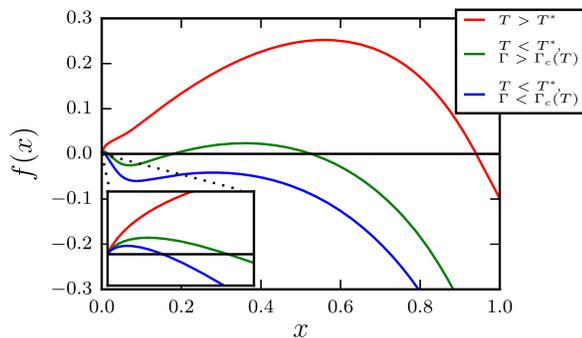ervable in the spin-glass theory is the Edwards-Anderson order parameter $q_{\text{EA}} \equiv (1/N)\sum_i \langle \sigma_i \rangle^2$, where the average is with respect to the Gibbs distribution. We define an eigenstate variant $q_{\text{ES}}(\Psi) \equiv (1/N)\sum_i \langle \Psi | \sigma_i^z | \Psi \rangle^2$. Note that $q_{\text{ES}}(\Psi) = q_{\text{EA}}$ whenever the ETH holds. Heuristically, $q_{\text{ES}}(\Psi)$ measures how similar the configurations are for which $|\Psi\rangle$ has a significant amplitude. $q_{\text{ES}}(\Psi) \sim 1$ means that measuring the σ^z configuration within state $|\Psi\rangle$ will consistently give macroscopically similar results. One can then associate a specific magnetization pattern to $|\Psi\rangle$. As shown in Ref. [43], Sec. G, in the nonergodic phase of H_p,

$$q_{\text{ES}} = 1 - \frac{4\Gamma^2 T^2}{p^2} + \cdots. \tag{9}$$

Compare to ergodic eigenstates in the paramagnetic phase, which have $q_{\text{ES}} = 0$.

The level statistics in the nonergodic phase is Poisson as well, just as in many-body-localized systems. Regardless of how the eigenstates hybridize within a cluster, they cannot do so over more than the total number of configurations in the cluster, which is $e^{N \exp(-p\epsilon_0^2)}$ (see [43], Sec. C). These levels strongly repel and have Gaussian Orthogonal Ensemble statistics, but the spacing between them scales no smaller than $e^{-N \exp(-p\epsilon_0^2)}$. Yet different clusters have independent fluctuations in energy levels, and the number of clusters is at least $e^{N[\ln 2 - \epsilon_0^2 - \exp(-p\epsilon_0^2)]} \gg e^{N \exp(-p\epsilon_0^2)}$. The spectra of different clusters interpenetrate, so the level statistics is Poisson. This is sketched in Fig. 4.

It is important to bear in mind that, although we give many analytic results only asymptotically in large p, the phenomenology that we have described here applies for *all* p, including those most likely to be experimentally realized ($p = 2, 3$) [48,49]. The existence of the nonergodic phase relies only on clustering in configuration space, which is
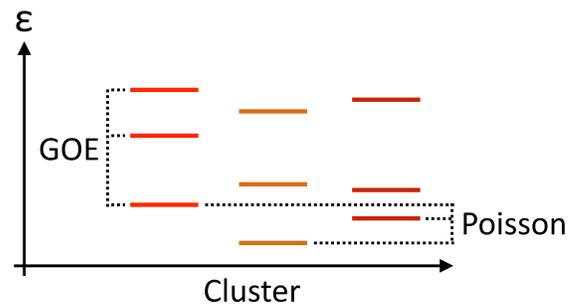

FIG. 3. The annealed entropy of resonances $f(x)$ (for $p = 20$). x is the fractional Hamming distance relative to an unperturbed state with energy density $\epsilon_0 = -(1/2T)$. The inset shows $f(x)$ at very small x. Red curve, $(T, \Gamma) = (2.27, 0.50)$. Green curve, $(T, \Gamma) = (1.56, 0.50)$. Blue curve, $(T, \Gamma) = (1.39, 0.50)$.

FIG. 4. A sketch of H_p's eigenvalues in the nonergodic phase (y axis), organized by the cluster to which each eigenstate belongs (x axis).

known to occur for all p [31,32,50]. The clustering phenomenon even extends beyond the p-spin models, making our results also relevant for, e.g., quantum annealing experiments on combinatorial optimization problems [16].

Since the nonergodic phase looks very similar to a many-body-localized phase, it raises the obvious question of how the two are related. The underlying physics is different: MBL is intrinsically a result of quantum interference, whereas the nonergodic phase is more a consequence of $O(N)$ energy and entropy barriers. In that respect, it relates more to the classical theory of glassiness in mean-field systems.

The relationship to the mean-field spin-glass theory, and, in particular, the replica theory [46,47], is potentially very deep. Most prominent is the connection between our T^* and the "dynamical" transition temperature T_d [27,32,53]. Below T_d, the Gibbs distribution concentrates around clusters in the configuration space (although the equilibrium properties may still be paramagnetic). The classical transition that we identify at T^* also corresponds to clustering in the configuration space, even though we have obtained it by independent means. The exact relationship between our calculations and the standard canonical analysis remains to be established, but, interestingly, Eq. (6) for the asymptotic-in-p behavior of T^* agrees exactly with T_d in the literature [54]. Furthermore, in Ref. [27], the authors studied H_p via the replica theory and found an entire curve $T_d(\Gamma)$, which in other models was shown to relate to real-time dynamics in the presence of a heat bath [55]. That transition lies above the nonergodic-ETH transition in Fig. 1; the connection between the two is an interesting open question.

On that note, it was recently argued [56] that ergodicity of eigenstates need not imply ergodicity of dynamics. It is possible that the decay time of classical states might diverge in the thermodynamic limit when $T < T^*$, even when the corresponding eigenstates are ergodic. If so, the thermodynamic curve $T_d(\Gamma)$ may describe the quench behavior of H_p rather than eigenstate properties.

And, finally, the intracluster structure of the nonergodic eigenstates may be very rich. The ultrametric structure of Parisi's solution [57] suggests that a cluster is organized into subclusters, which themselves have subclusters, and so on. The nonergodic phase may actually be many different phases, with varying degrees of ergodicity breaking corresponding to how many levels of clusters the eigenstates tunnel through, analogous to the physical picture of replica-symmetry breaking.

[1] B. L. Altshuler, Y. Gefen, A. Kamenev, and L. S. Levitov, Phys. Rev. Lett. **78**, 2803 (1997).

[2] D. Basko, I. Aleiner, and B. Altshuler, Ann. Phys. (Amsterdam) **321**, 1126 (2006).

[3] V. Oganesyan and D. A. Huse, Phys. Rev. B **75**, 155111 (2007).

[4] A. Pal and D. A. Huse, Phys. Rev. B **82**, 174411 (2010).

[5] M. Serbyn, Z. Papić, and D. A. Abanin, Phys. Rev. Lett. **111**, 127201 (2013).

[6] D. A. Huse, R. Nandkishore, and V. Oganesyan, Phys. Rev. B **90**, 174202 (2014).

[7] J. A. Kjäll, J. H. Bardarson, and F. Pollmann, Phys. Rev. Lett. **113**, 107204 (2014).

[8] M. Schreiber, S. S. Hodgman, P. Bordia, H. P. Lüschen, M. H. Fischer, R. Vosk, E. Altman, U. Schneider, and I. Bloch, Science **349**, 842 (2015).

[9] A. Altland and T. Micklitz, arXiv:1609.00877 [Phys. Rev. Lett. (to be published)].

[10] F. Ladieu, M. Sanquer, and J. P. Bouchaud, Phys. Rev. B **53**, 973 (1996).

[11] M. Ovadia, D. Kalok, I. Tamir, S. Mitra, B. Sacépé, and D. Shahar, Sci. Rep. **5**, 13503 (2015).

[12] J. Smith, A. Lee, P. Richerme, B. Neyenhuis, P. W. Hess, P. Hauke, M. Heyl, D. A. Huse, and C. Monroe, Nat. Phys. **12**, 907 (2016).

[13] G. Kucsko, S. Choi, J. Choi, P. Maurer, H. Sumiya, S. Onoda, J. Isoya, F. Jelezko, E. Demler, N. Yao, and M. Lukin, arXiv:1609.08216.

[14] S. Choi, J. Choi, R. Landig, G. Kucsko, H. Zhou, J. Isoya, F. Jelezko, S. Onoda, H. Sumiya, V. Khemani, C. von Keyserlingk, N. Y. Yao, E. Demler, and M. D. Lukin, arXiv:1610.08057.

[15] M. W. Johnson *et al.*, Nature (London) **473**, 194 (2011).

[16] S. Boixo, T. F. Rønnow, S. V. Isakov, Z. Wang, D. Wecker, D. A. Lidar, J. M. Martinis, and M. Troyer, Nat. Phys. **10**, 218 (2014).

[17] S. Boixo, V. N. Smelyanskiy, A. Shabani, S. V. Isakov, M. Dykman, V. S. Denchev, M. H. Amin, A. Y. Smirnov, M. Mohseni, and H. Neven, Nat. Commun. **7**, 10327 (2016).

[18] P. W. Anderson, Phys. Rev. **109**, 1492 (1958).

[19] D. E. Logan and P. G. Wolynes, J. Chem. Phys. **87**, 7199 (1987).

[20] L. Levitov, Ann. Phys. (Berlin) **8**, 697 (1999).

[21] N. Y. Yao, C. R. Laumann, S. Gopalakrishnan, M. Knap, M. Müller, E. A. Demler, and M. D. Lukin, Phys. Rev. Lett. **113**, 243002 (2014).

[22] A. L. Burin, Phys. Rev. B **91**, 094202 (2015).

[23] C. R. Laumann, A. Pal, and A. Scardicchio, Phys. Rev. Lett. **113**, 200405 (2014).

[24] C. L. Baldwin, C. R. Laumann, A. Pal, and A. Scardicchio, Phys. Rev. B **93**, 024202 (2016).

[25] Y. Y. Goldschmidt, Phys. Rev. B **41**, 4858 (1990).

[26] T. M. Nieuwenhuizen and F. Ritort, Physica A (Amsterdam) **250A**, 8 (1998).

[27] L. F. Cugliandolo, D. R. Grempel, G. Lozano, and H. Lozza, Phys. Rev. B **70**, 024422 (2004).

[28] T. Jörg, F. Krzakala, J. Kurchan, and A. C. Maggs, Phys. Rev. Lett. **101**, 147204 (2008).

[29] B. Derrida, Phys. Rev. Lett. **45**, 79 (1980).

[30] D. Gross and M. Mezard, Nucl. Phys. **B240**, 431 (1984).

[31] E. Gardner, Nucl. Phys. **B257**, 747 (1985).

[32] T. R. Kirkpatrick and D. Thirumalai, Phys. Rev. B **36**, 5388 (1987).

[33] D. Sherrington and S. Kirkpatrick, Phys. Rev. Lett. **35**, 1792 (1975).

[34] G. Parisi, Phys. Rev. Lett. **43**, 1754 (1979).

[35] G. Biroli, A. C. Ribeiro-Teixeira, and M. Tarzia, arXiv:1211.7334.

[36] A. De Luca, B. L. Altshuler, V. E. Kravtsov, and A. Scardicchio, Phys. Rev. Lett. **113**, 046806 (2014).

[37] B. L. Altshuler, E. Cuevas, L. B. Ioffe, and V. E. Kravtsov, Phys. Rev. Lett. **117**, 156601 (2016).

[38] J. M. Deutsch, Phys. Rev. A **43**, 2046 (1991).

[39] M. Srednicki, Phys. Rev. E **50**, 888 (1994).

[40] M. Rigol, V. Dunjko, and M. Olshanii, Nature (London) **481**, 224 (2008).

[41] M. Srednicki, J. Phys. A **32**, 1163 (1999).

[42] F. Pietracaprina, V. Ros, and A. Scardicchio, Phys. Rev. B **93**, 054201 (2016).

[43] See Supplemental Material at http://link.aps.org/supplemental/10.1103/PhysRevLett.118.127201 for detailed derivations of these results.

[44] M. Mézard, T. Mora, and R. Zecchina, Phys. Rev. Lett. **94**, 197205 (2005).

[45] R. Mulet, A. Pagnani, M. Weigt, and R. Zecchina, Phys. Rev. Lett. **89**, 268701 (2002).

[46] M. Mézard, G. Parisi, and M. Virasoro, *Spin Glass Theory and Beyond*, Lect. Notes Phys. (World Scientific, Singapore, 1987).

[47] M. Mézard and A. Montanari, *Information, Physics, and Computation*, Oxford Graduate Texts (Oxford University, New York, 2009).

[48] P. Strack and S. Sachdev, Phys. Rev. Lett. **107**, 277202 (2011).

[49] S. Gopalakrishnan, B. L. Lev, and P. M. Goldbart, Phys. Rev. Lett. **107**, 277201 (2011).

[50] Numerical studies, e.g., exact diagonalization, could provide an important validation, yet for small p one needs very large N to separate the various features. Current state-of-the-art techniques are limited to $N \approx 30$ [51,52], which is too small.

[51] D. J. Luitz, N. Laflorencie, and F. Alet, Phys. Rev. B **91**, 081103 (2015).

[52] A. Lerose, V. K. Varma, F. Pietracaprina, J. Goold, and A. Scardicchio, arXiv:1511.09144.

[53] H. Sompolinsky and A. Zippelius, Phys. Rev. Lett. **47**, 359 (1981).

[54] U. Ferrari, Ph.D. thesis, Universita di Roma, 2012.

[55] L. F. Cugliandolo, D. R. Grempel, and C. A. da Silva Santos, Phys. Rev. B **64**, 014403 (2001).

[56] A. Chandran, A. Pal, C. Laumann, and A. Scardicchio, Phys. Rev. B **94**, 144203 (2016).

[57] M. Mézard, G. Parisi, N. Sourlas, G. Toulouse, and M. Virasoro, Phys. Rev. Lett. **52**, 1156 (1984).